Heritage Science

RESEARCH

Open Access

A case study investigation-based experimental research on transport of moisture and salinity in semi-exposed relics

Yike Wang[1,2], Jiaxuan Li[2], Yin Xia[2,3], Bin Chang[2] and Xilian Luo[2*]

Abstract

Semi-exposed relics within an air–soil system often have earthworks partially buried, leading to moisture migration and substantial salt accumulation. Salt accumulation threatens relic preservation, but destructive sampling is hindered by conservation concerns. We conducted a case study on salt enrichment at K9901 Armour Pit of Emperor Qinshihuang 's Mausoleum Site Museum. Environmental factors and soil salt characteristics were assessed through sampling and monitoring. A relic-soil coupling system was established with a soil column device containing burned bricks. Using 5-TE sensors, water and salinity movement was tracked, and X-ray diffraction analyzed relic salt crystals. The soil column experiment effectively simulated water-salt migration in relics. Salts, like Cl^-, NO_3^-, SO_4^{2-}, Na^+, and Mg^{2+}, concentrated on the soil surface during evaporation. Simulation linked specific salt species to relic ailments. Salt solution from soil migrated to bricks, forming $CaSO_4$ crystals. Results highlight coupling's role in salt-related deterioration and the need to protect it for optimal relic preservation. Findings impact semi-exposed relic conservation, revealing salt accumulation processes and their impact on historical artifacts.

Keywords Semi-exposed relics, Soil column experiment, Salt migration

Introduction

Earthen sites hold immense cultural heritage value as they preserve traces of human historical activities, offering invaluable insights for both scientific inquiry and cultural education [1]. China is endowed with a rich collection of earthen sites, boasting more than 1250 of them designated as national key earthen site protection units [2]. This constitutes a significant 25% of the total number of cultural relics granted primary protection status [3]. Regrettably, a multitude of these earthen sites are grappling with a range of challenges. These include threats such as wind and sand erosion [4], intense rain-induced erosion [5], drought-induced shrinkage [6], freeze–thaw cycles [7], seismic events [8], biological weathering [9], and human-induced activities [10]. Hence, safeguarding these relics necessitates immediate action to preserve these earthen sites and prevent their degradation.

As delineated by Gu et al. [11], museums dedicated to heritage conservation can be broadly classified into two primary categories. The first category pertains to museums predominantly engaged in showcasing movable artifacts. Conversely, the second category encompasses archaeological museums that revolve around the conservation of immovable historical sites. Artifacts showcased in museums with a focus on display are typically safeguarded within enclosed display cases. On the other hand, historical sites like the Egyptian pyramids or the Great Wall of China stand as tangible remnants of past human activities and are often directly exposed to the open atmosphere. These sites face imminent and

*Correspondence:
Xilian Luo
xlluo@mail.xjtu.edu.cn
[1] Institute of Geographic Sciences and Natural Resources Research, Chinese Academy of Sciences, Beijing 100101, China
[2] School of Human Settlements and Civil Engineering, Xi'an Jiaotong University, Xi'an 710049, China
[3] Emperor Qinshihuang's Mausoleum Site Museum, Xi'an 710600, China

substantial threats of degradation, driven by fluctuations in climate, environmental contamination, and human activities [12]. An efficacious strategy for preserving these small-scale, unmovable historical sites involves the construction of archaeological museums around them [13].

With the extensive progression of archaeological endeavors and the continuous advancement of technology for safeguarding cultural relics, China boasts a repertoire of over 3000 museums, with a substantial portion of these being archaeology museums [14]. For enhanced accessibility in terms of exhibition and preservation, subterranean earthen sites have been meticulously unearthed and are now presented to visitors in a semi-exposed setting (Fig. 1a) [15]. However, alongside these developments, Luo et al. [6] revealed that the movement of water from within the soil towards the surface layer is inherently spontaneous and unidirectional. The manifestation of salt-induced damage predominantly occurs subsequent to the excavation of earthen sites, owing to the alteration of their storage environment from deep, saturated soil to a state characterized by the interplay of soil, relics, and air (Fig. 1b) [16]. In this transformed state, water within the soil migrates towards the surface, subsequently evaporating. Concurrently, soluble salts in the soil embark on a parallel journey towards the earthen site's surface alongside the water's transport. This intricate process eventually culminates in the accumulation of salts on the earthen site's surface [17].

Emperor Qinshihuang 's Mausoleum Site Museum, renowned for its grandeur and unparalleled collection of buried artifacts among ancient imperial mausoleums in China, attained UNESCO's recognition as a World Heritage Site in 1987. Within the museum, over 600 earthen sites, encompassing funerary pits and accompanying tombs, have been unveiled [18]. Despite their unearthing, these earthen sites are presently undergoing a process of degradation, primarily attributable to the enrichment of salts on their surfaces [19]. This pattern of deterioration is not unique to this museum; it extends to other significant heritage sites as well. For instance, the Yungang Grottoes, which house approximately 50,000 stone relics, have encountered various forms of affliction. Among these, a predominant issue involves the impairment of rock formations, inclusive of rock carvings. This impairment stems from the crystallization pressure of salts within the interstices and pores of the rocks, exerting a disruptive influence on their structural integrity [20, 21]. Meanwhile, at another distinguished World Heritage Site, the Mogao Grottoes, a collection of murals has exhibited signs of rapid deterioration within a mere few decades, primarily due to salt accumulation [22]. This process of degradation is marked by recurrent cycles of salt dissolution, accompanied by subsequent swelling and crystalline contraction. This dynamic flux of soluble salts ultimately leads to the disintegration, loosening, detachment, or gradual dispersion of pigments within the artworks [23].

Numerous researchers have dedicated their efforts to addressing the challenge of salt-related damage in earthen sites. A multitude of studies have been conducted in this pursuit. Through on-site investigations, Arnold et al. [24] meticulously examined the type of salts present and their corresponding levels of damage across distinct heights on walls. They concluded that the distribution of

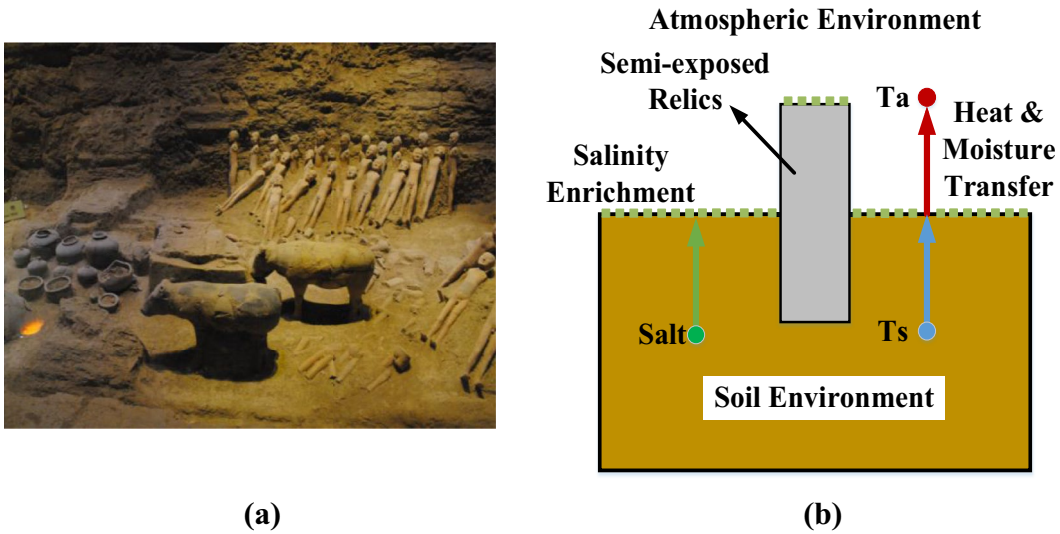

Fig. 1 Image of the heritage site and diagram of the half-exposed relics. **a** semi-exposed relics in museum **b** schematic diagram of the semi-exposed relics

salts is closely linked to their solubility. Steiger et al. [25] extended this exploration by delving into the salt content and enrichment patterns on walls across multiple sites in northern Bavaria and other monuments. Regarding the intricate process of salt migration, Russo et al. [26] proposed an innovative approach through a soil column experiment. This experiment involved monitoring moisture content and conductivity at different depths utilizing sensor probes. Russo's research revealed that concentrations of Na^+, Mg^{2+}, Ca^{2+}, Cl^-, and SO_4^{2-} exhibited synchronized fluctuations with salinity at various depths. However, a more comprehensive investigation is essential to determine the feasibility of applying the soil column experiment to accurately simulate the complex soil-relic coupling system characteristic of semi-exposed relics and their associated salt enrichment processes.

This study endeavors to achieve three primary objectives. Firstly, it aims to investigate the distribution of salinity and soil characteristics at varying depths within the K9801 armor pit situated at Emperor Qinshihuang 's Mausoleum Site Museum. Secondly, the study seeks to establish soil column experiments, facilitating the real-time observation of soil water and salt migration. By comparing the resulting salt distribution with that observed within the K9801 armor pit, the study intends to validate the suitability of soil column experiments for emulating the intricate water and salt migration processes. Lastly, through the application of destructive sampling on simulated semi-exposed brick within soil columns, the study aspires to dissect the mechanisms underpinning salt enrichment in semi-exposed relics.

Materials and methods

K9801 armour pit in Emperor Qinshihuang 's Mausoleum Site Museum investigation

Emperor Qinshihuang 's Mausoleum Site Museum stands as one of China's most renowned site museums, situated on the grounds of the funerary pit sites of Emperor Qinshihuang 's Mausoleum Site Museum. Its inauguration occurred in 1979, subsequently earning UNESCO's endorsement in 1987 for inclusion in the esteemed World Heritage List [27]. Figure 2 visually depicts the layout of preservation and excavation zones within Emperor Qinshihuang 's Mausoleum Site Museum complex. Spanning an expanse of 3.2 square kilometers, the protected area encompasses six excavated funerary pits: No. 1 pit, No. 2 pit, No. 3 pit, K0006 funerary pit, K9901 funerary pit, and the K9801 armour pit. Exhibition halls have been meticulously constructed for the first five pits, thereby welcoming tourists to explore their historical treasures. The the K9801 armour pit, however, currently remains in the phase of archaeological excavation and preservation evaluation.

The K9801 Armor pit, unearthed in 1998 between the inner and outer precincts of the Mausoleum of the First Qin Emperor (MFQE), stands as a remarkable

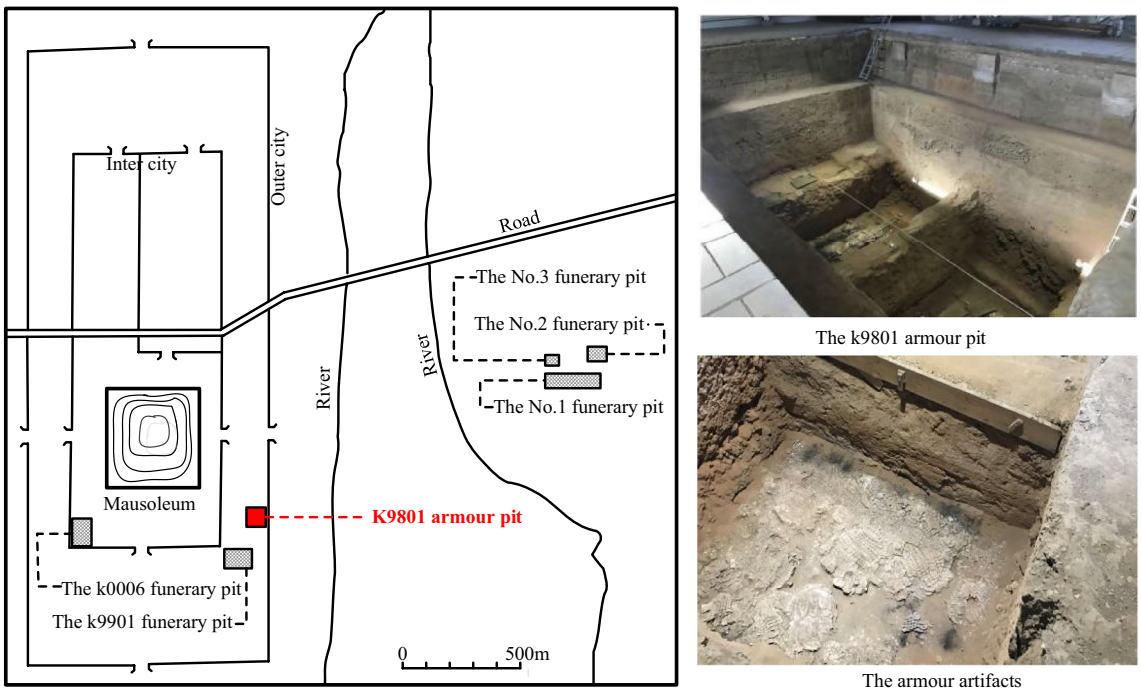

Fig. 2 K9801 armour pit of Emperor Qinshihuang 's Mausoleum Site Museum

archaeological discovery. This pit, situated in the southeastern part of the complex, holds an extensive assortment of stone armor and helmets, as depicted in Fig. 2 [28]. Spanning an impressive 129 m in its east–west dimension and 105 m from north to south, this pit claims the distinction of being the most expansive burial pit within Emperor Qinshihuang 's Mausoleum Site Museum. It harbors a multitude of interred sites containing armor, stone horse reins, and other invaluable relics. Notably, the pit also reveals a substantial number of architectural remnants within its compacted earth walls, as illustrated in Fig. 2b. Structurally, the K9801 armor pit assumes the form of an underground tunnel-type civil structure with a distinctive "convex" configuration in its plane.

Backed by the endorsement of the Ministry of Science and Technology of the People's Republic of China and the State Administration of Cultural Heritage, Emperor Qinshihuang 's Mausoleum Site Museum is poised to implement an air curtain system. This innovative system is envisioned to establish a meticulously controlled and hygienic preservation environment for the historical treasures situated within the stone armor pit. This endeavor aligns with the museum's aspiration for a "clean and stable" conservation setting [27]. The primary goal of the survey conducted in this study was to shield the relics from the detrimental effects of salinity. Consequently, the survey focused solely on the sampling of soil from the sealing layer, carefully avoiding any potential harm to the site itself. Notably, considering that the K9801 Armor pit remains in the process of archaeological excavation and conservation assessment, this survey was meticulously designed to ensure that it did not disrupt the ongoing conservation endeavors and tourist activities.

The study employed samples sourced from diverse locations within the K9801 Armor pit, as illustrated in Fig. 3. The sampling strategy encompassed the second step of the pit, where soil samples at varying depths were procured and designated as PY-1 through PY-9. To elaborate, the topmost 5 cm of soil was subjected to sampling at 1-cm intervals, leading to the assignment of PY-1 through PY-5. Subsequently, sampling extended to depths ranging from 0.2 to 0.8 m, with 20-cm intervals, leading to the allocation of PY-6 through PY-9. The sampled soil masses ranged from 10 to 50 g. It's noteworthy that samples obtained at the same depth from distinct regions were combined post-sampling, resulting in mixed samples for further analysis.

Construction of soil column experiment

Soil specimens were meticulously gathered from a foundation pit situated outside the Heritage Conservation Area in Xi'an, Shaanxi province. These samples were extracted from a depth of 8 to 10 m and correspond to

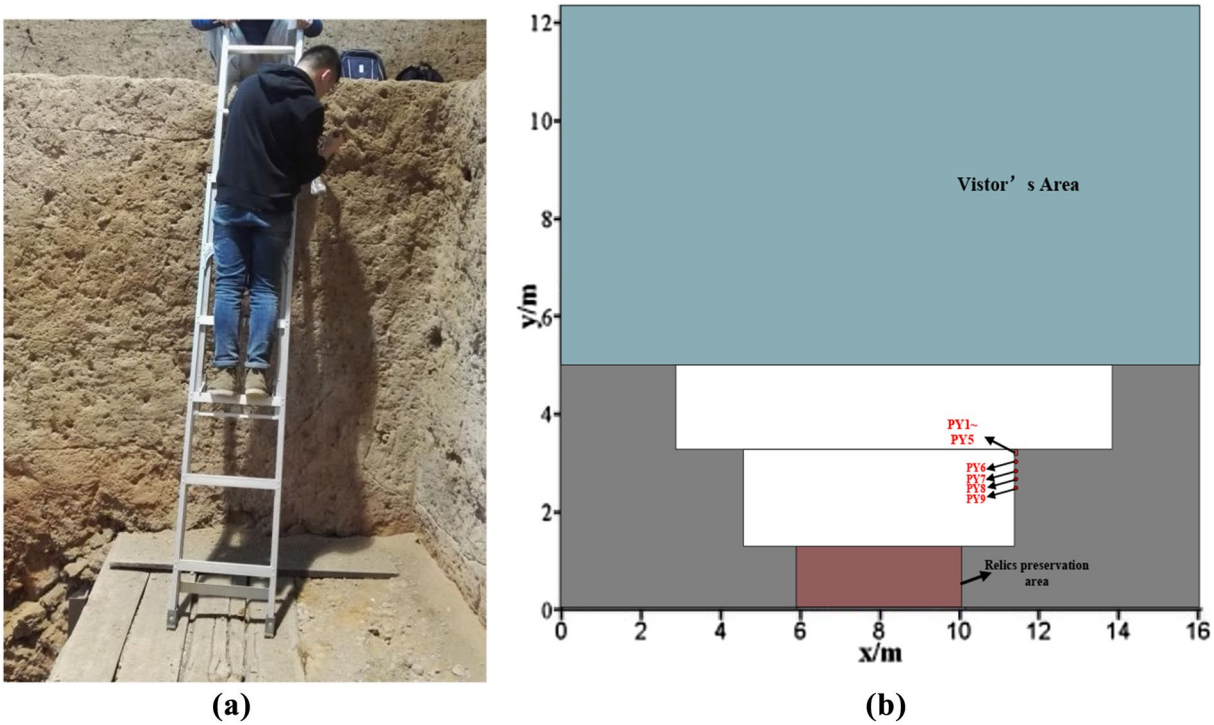

Fig. 3 The Sampling site in K9801 armour pit. **a**The sampling process; **b** Central section of the K9801 Armour pit

Table 1 The soil texture of experimental soil column device

Particle-size distribution/%				Bulk density/ kg·m − 3	Porosity degree/%
1–2 mm	0.02–1 mm	0.002–0.02 mm	< 0.002 mm		
0.11	73.15	25.77	1.07	1630	42.11

Fig. 4 Photograph of the experimental brick

the late Pleistocene (Q3) loess strata, a geological era previously elucidated by Xu et al. [29]. The unblemished soil samples were excised from the sidewall of the foundation pit. In order to ascertain the fundamental physical characteristics of the soil, standard geotechnical testing protocols were adhered to (GB/T50123-2019, 2019). The comprehensive results of these tests have been compiled and are provided in Table 1.

The brick (24 cm length × 3 cm width × 10 cm high) is crafted from kiln clay and the locally sourced brownish red clay. This brick, formed through a premanufacturing process and subsequently fired with approximately 20% sand content, emulates the firing technique employed for creating the famed terracotta warriors. Notably, these bricks were meticulously chosen to serve as representative specimens of the cultural relics housed within the Terracotta Warriors and Horses Museum, as visually depicted in Fig. 4.

The vertical soil column test system comprises a plexiglass soil column, a Markov bottle water supply mechanism, and a monitoring apparatus, as depicted in Fig. 5. Transparent polymethyl methacrylate (PMMA) cylinders were employed as the soil columns, measuring 30 cm in diameter and 100 cm in height, with small apertures at the base (Fig. 5). Preceding the soil filling process, a 5-cm-thick filter paper was positioned at the base of each cylinder. To ensure uniform soil bulk density (1.35 g cm^{-3}), the dry, sieved soil was progressively added to each column in 10-cm increments. Before the subsequent layer was introduced, the soil surface of the previously packed layer was gently agitated to forestall any stratification. Each column was filled up to a height of 100 cm. For the purpose of tracking the infiltration front, a 100-cm-long measuring tape was affixed vertically to

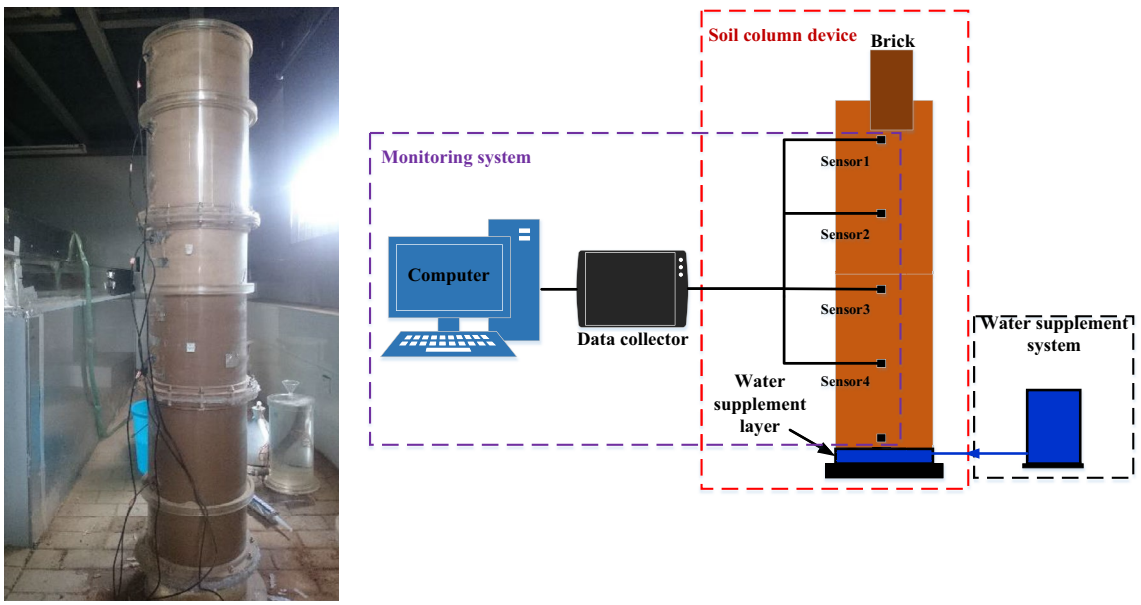

Fig. 5 The vertical soil column test system. **a** Photograph of the soil column device; **b** Diagram of the soil column device

the outer wall of every soil column. In emulating semi-exposed relics, the brick was positioned at a depth of 12 cm within the soil column, while the remaining portion of the brick remained exposed to the air. This configuration was designed to simulate the conditions of such semi-exposed artifacts.

Monitoring system

The monitoring system for soil temperature, water content, and electrical conductivity encompassed 5TE sensors, with their respective parameters detailed in Table 2. This system was integrated with an EM50 data collector, ECH2O acquisition software, and a computer to facilitate data collection and analysis.

The sensors were strategically situated at distances of 20, 40, 60, and 80 cm from the soil column's surface. These sensors were programmed to capture data at intervals of 20 min.

The 5TE sensor laboratory calibration followed the procedure outlined by J.L. Varble and J.L. Chávez [30]. Briefly, water content was calculated by multiplying the gravimetric water content with the soil bulk density from the field and then dividing by the density of water. The samples were subsequently packed into 19L containers to mimic field soil bulk density. The soil in the container was subsequently wetted with 500 mL of water and thoroughly mixed. This procedure was iteratively repeated, involving repacking the container, acquiring multiple sensor readings, and adding 500 mL of water until the soil water content approached field capacity. Eight gravimetric soil samples (n = 6) were used in the analysis of the soil samples.

Bulk soil electrical conductivity depends both on the concentration of salts in the soil and the volumetric water content. The previous testing procedures on the water content sensors were repeated, and an addition of salts to the soil samples, different concentrations of calcium chloride dihydrate solutions were mixed thoroughly with the soil. Tests on the soils were then conducted in the manner previously mentioned. A total of eight samples were used to calibrate the 5TE sensors' water content and electrical conductivity. The temperature of the soil in the laboratory tests was relatively constant (~25 C, ~40 C) throughout the entire study.

Experimental cases

Details of the test conditions are given in Table 3.

Sampling

Subsequent to the Acceleration stage on May 20, 2022, samples were procured from both the soil columns and the brick specimens. Soil sampling encompassed two distinct ranges: the top 5 cm of the column surface and the depth interval of 20 to 80 cm. For the top 5 cm of the column surface, sampling transpired at 1-cm intervals, designated as MN 1–5. Meanwhile, within the 20 to 80 cm depth range, sampling transpired at depths of 20, 40, 60, and 80 cm, assigned as MN 6–9 (Fig. 6a). Approximately 10–15 g of soil were collected at each depth, involving multiple samples that were subsequently combined.

In terms of brick sampling, a distinct strategy was employed. Sampling occurred at intervals of 4 cm within the 0 to 24 cm range, labeled as A ~ H (as illustrated in Fig. 6b. Furthermore, salt crystals present on the brick surfaces were also harvested through brush collection. Samples were sampled after the 5/20/2022 Acceleration stage and were sampled from soil in soil columns and brick.

Table 2 The parameters of 5TE soil temperature, moisture and electrical conductivity sensor

Measurement parameter	Volumetric water content	Electrical conductivity/dS·m − 1	Temperature/°C
Precision	± 3%	0.02	± 1
Resolution	0.08% (0–50%)	0.05 (7–23.1)	0.1
Measuring range	0–100%	0–23.1	−40–50

Table 3 Experimental conditions

Stages	Description	Duration
1: Hydration stage	Supply of water and use of plastic wrap to reduce evaporation	3/30/2022–4/20/2022
2: Stable stage	Supply of water and no plastic wrap	4/20/2022–5/2/2022
3: Acceleration stage	No water supply, no plastic wrap, Raising the temperature	5/2/2022–5/20/2022

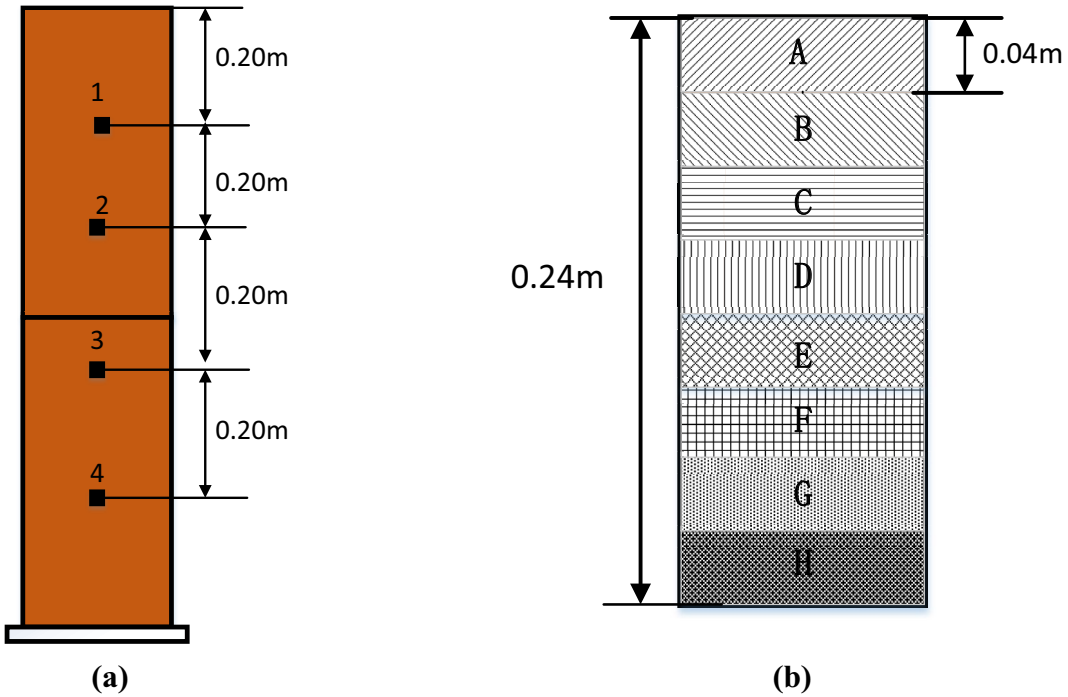

Fig. 6 Schematic diagram of the sampling points in the column. **a** Soil column sampling point; **b** Brick sampling point

Determination of salt crystals

The mineralogical understanding of building materials is indispensable to studying the preservation and restoration of architectural heritage sites [10]. The mineral compositions of the blue bricks were identified by powder X-ray diffraction (XRD) using an X-ray diffractometer (D/max-2500/PC, Rigaku, Japan) with Cu Kα1 radiation (λ = 1.54 Å). The following conditions were used for the test: a voltage of 35 kV, a current intensity of 50 mA, an explored 2θ range between 2° and 70°, a step size of 0.020° (1.2 s) and a scan speed of 1.000°min^{-1}. Each sample was ground separately until all of the particles passed through a sieve with 0.063 mm mesh.

Determination of soil salt ions

0.2g soil samples were dissolved in 50 ml deionized water with accelerated stirring and sonicated for 30 min.The supernatant was centrifuged and analysed by ion chromatography (Diane ICA-90 Research Ion Chromatograph, USA). The content of each ion in the soil site was calculated as Eq. (1):

$$Q(mg\backslash g) = \frac{C}{D} \tag{1}$$

where, Q is the ion content,mg g-1; C is the ion content of the sample measured in 50 ml of deionized water, mg; G is the mass of the soil sample taken from the site, g.

Results and discussion

Verification of soil column experiment

To verify whether the addition of semi-exposed relics has an effect on salt transport in the soil column experiment, by comparing the concentrations of different types of salts at different depths in the K9801 Armour pit and soil column.

The soil column experiment effectively replicated the salt distribution pattern within semi-exposed relics. Predominantly, salt ions were concentrated within the surface layer of 0–5 cm, displaying comparatively lower concentrations in the 20–80 cm range (Fig. 7). This observation aligns with the one-way migration theory advanced by Luo et al. [6], postulating that solely regulating external air humidity cannot entirely counteract the water migration from soil to air. This unidirectional migration, consequently, results in the accumulation of soluble salts at the soil's surface. To enhance the specificity of our findings to the unique conditions of the K9801 burial pit, we conducted a more detailed analysis of the salt enrichment process. Our examination uncovered salt accumulation in the K9801Armour pit, notably occurring

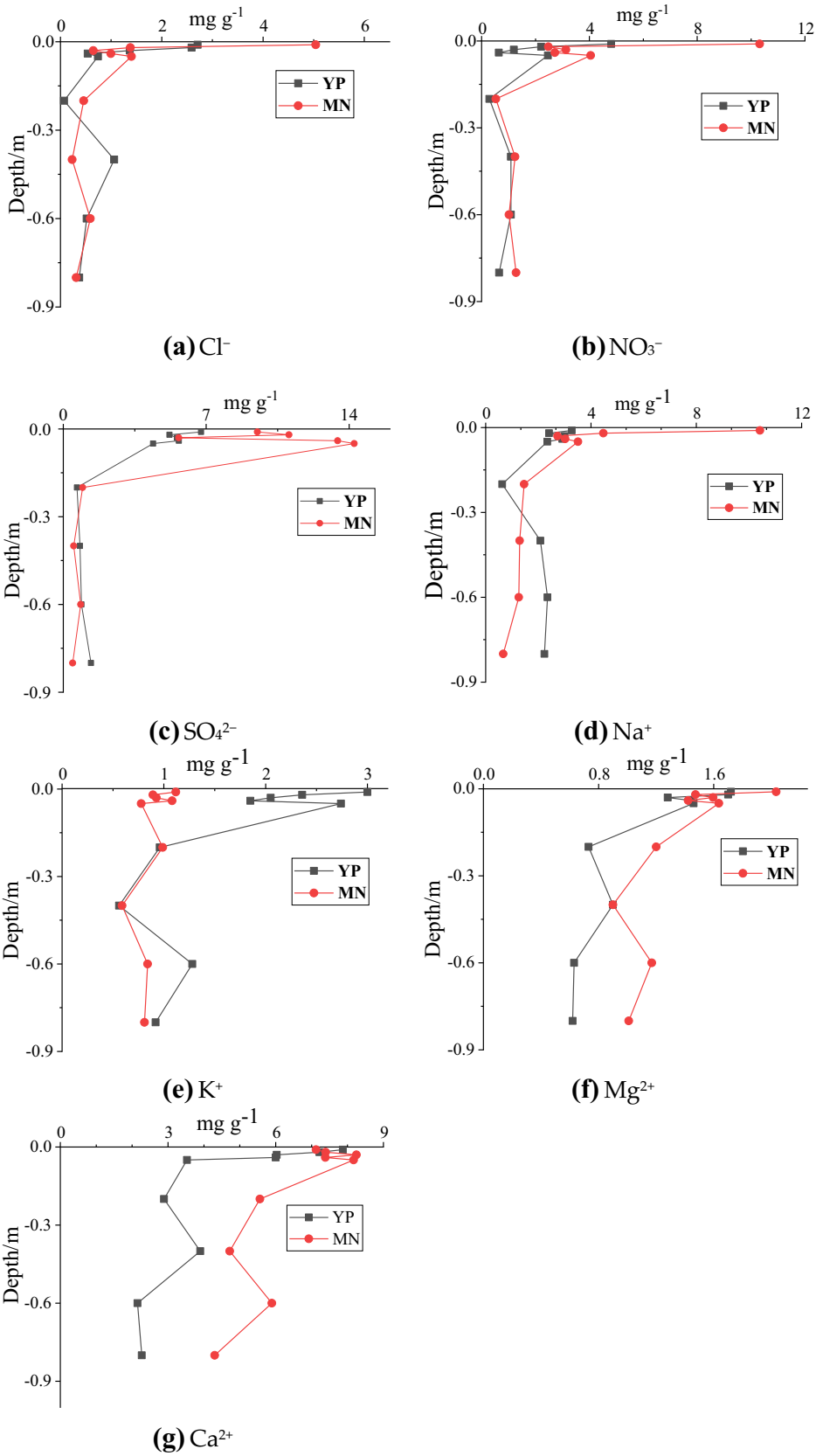

Fig. 7 Changes in the content of soil ions at different depths

at a depth of 0–20 cm, with the concentration at 0–5 cm significantly surpassing the simulated surface salt concentration of the soil column (Fig. 7). Simultaneously, the outcomes of the soil column experiment on salt enrichment correspond well with the findings of Xu et al. [29]. As the accumulation of crystals persists, the ascent of the salt solution accelerates, leading to an augmented concentration of salt crystals within surface areas.

Nevertheless, in contrast to the trend of salt transportation, the enrichment patterns of distinct salt ions from short-term soil column simulations diverged from those observed in the K9801 armour pit (Fig. 7). Specifically, for Cl^-, NO_3^-, SO_4^{2-}, Na^+, and Mg^{2+}, the distribution of salt ions at depths of 0.2–0.8 m in the soil column experiments mirrored the salt concentration at identical depths in the K9801 armour pit. However, the salt content at the surface of the K9801 armour pit was marginally lower than that predicted by the simulated soil column (Fig. 7).

To delve deeper into these disparities, we explored the unique characteristics of the K9801 burial pit. Our findings revealed that the enrichment patterns of Cl^-, Na^+, and other constituents are in alignment with Xia et al.'s research [31]. The presence of a curing-salt-laden colloidal substance with smooth edges and shrinkage holes containing Cl^-, NO_3^-, SO_4^{2-}, Na^+, K^+, Ca^{2+}, etc., in pottery efflorescence exhibits a similarity in salt enrichment status. However, discrepancies emerge in the distribution of K+and Ca2+in the simulated soil column as compared to the K9801 Armour pit, particularly at depths of 0.2–0.8 m, where the soil column samples exhibit higher salt concentrations(Fig. 7). Notably, the divergence might be attributed to the fact that the K9801 armour pit was sampled from the second terrace, which is distinct from the genuine soil surface (Fig. 3). This nuanced difference in sampling locations contributes to the variation in salt distribution at the surface.

Furthermore, Du et al. [28] propose that changes in K^+ content within the soil are influenced by both water migration and soil adsorption. Discrepancies in Ca^{2+} distribution could potentially be attributed to soil crystals. Primary carbonate minerals in Chinese loess are predominantly calcite and dolomite, while secondary carbonates like calcium carbonate are formed through weathering and leaching [29], potentially explaining the elevated distribution of Ca^{2+}. These nuanced differences underscore the importance of considering the specific characteristics of archaeological sites, such as the K9801 burial pit, to gain a comprehensive understanding of salt enrichment patterns and their implications for relic preservation.

Moisture and salinity transformation in soil

Figures 8 and 9 show the change in moisture content and electrical conductivity in vertical soil columns.

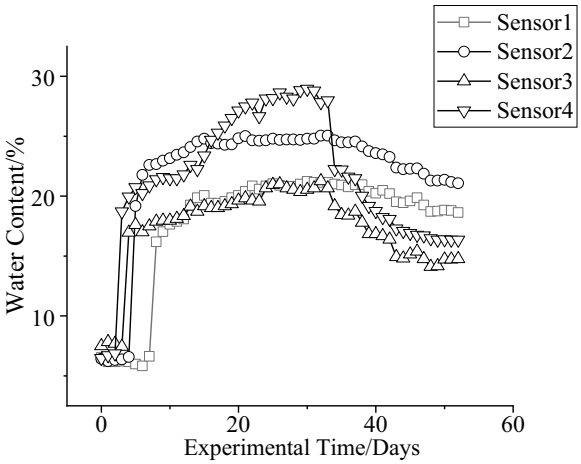

Fig. 8 Variation of soil moisture content with time at different depths of the soil column

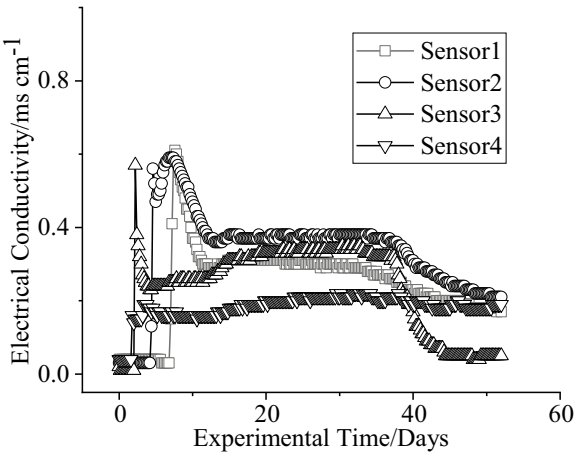

Fig. 9 Variation of soil electrical conductivity with time at different depths in the soil column

The experiment utilized air-dried soil, resulting in a low initial moisture content, as shown in Fig. 8. This initial condition was selected to simulate conditions similar to those encountered in archaeological sites, such as the K9801 armour pit. The K9801 armour pit, with its specific environmental characteristics, is prone to low initial moisture content due to factors like weathering and limited exposure.

During the hydration stage, the predominant factor influencing electrical conductivity was the water content, as depicted in Fig. 9. As the soil's water content increased in the hydration stage, the electrical conductivity exhibited an upward trend, subsequently stabilizing gradually (Fig. 9). This aligns with the observations in the K9801 burial pit; during the early

excavation phase, fluctuations in precipitation and seasonal groundwater changes induce variations in moisture content. Understanding these fluctuations is crucial for interpreting the conductivity patterns observed in both experimental and actual burial pits.

The gradual decrease observed after the electrical conductivity reached its peak was a consequence of soil salinity migration. Salts followed the peak of infiltration and underwent continuous enrichment. With the completion of the protective structure for K9801Armour pit, rainfall sources for moisture were severed. Salts, as observed in the K9801 armour pit, undergo unidirectional migration through the evaporative process. Peaks in electrical conductivity during the hydration stage in both the experiment and the burial pit highlight the intricate relationship between water content and salt dynamics.

Consequently, during the hydration stage, peaks were evident in all sensors. However, as the infiltration peak continued to rise, highly soluble salts were carried away, leading to a gradual reduction in the electrical conductivity of the sensors. This phenomenon corresponds to observations made in the K9801 burial pit (Fig. 7), where continuous enrichment and migration of salts play a pivotal role in shaping the overall salinity profile.

As the infiltration peak transported a significant amount of salt to the soil surface, accompanied by increased evaporation, crystallization commenced on the surface of both the soil and the brick. The precipitated salt crystals attracted additional water, resulting in its upward migration. This upward water movement, akin to what may occur in the K9801 armour pit under specific environmental conditions, led to the deposition of soluble salts on both the experiment and the K9801 armour pit soil surface. This phenomenon is also corroborated in the studies conducted by Chang et al.[19] and Xu et al. [29] through their Hydrus simulations, where salts were transported along with water, followed by enrichment and eventual stabilization after a certain period of time.

During the hydration stage, the observed upward migration of soil water and salt in the experimental setup parallels the potential dynamics in the K9801 armour pit. Given the low initial moisture content, water and salts move from the base of the soil column towards the surface, mirroring the conditions in the archaeological site.

As the soil column reached saturation, the continued slow migration of water upwards reflects a replenishing process, akin to the potential replenishment of moisture in the K9801 armour pit. This process, influenced by evaporation and subsequent rehydration, sheds light on how environmental factors could impact the semi-exposed relics, considering the specific conditions of the archaeological context.

Concurrently, the migration of salt towards the soil surface aligns with what might occur in the K9801 armour pit. The experiment's findings regarding the increased salt concentration on the soil surface during evaporation resonate with potential scenarios in the archaeological site, highlighting the interconnected nature of water and salt dynamics in semi-exposed relics.

Subsequently, in the accelerated evaporation stage, The general reduction in soil water content and electrical conductivity provides insights into how environmental conditions in the K9801 armour pit, such as potential fluctuations in humidity and temperature, may contribute to the tendency for salt accumulation on the surface of artifacts or archaeological sites. This comparative analysis provides a valuable perspective on the experimental results, offering a plausible connection between the observed soil column behavior and the potential processes influencing the K9801 armour pit. By drawing parallels, the study contributes to a more comprehensive understanding of how salt migration and hydration dynamics manifest in the specific context of semi-exposed relics, such as the K9801 armour pit.

The effect of salt on simulated cultural relics

The utilization of half-buried bricks within the soil column experiment, specifically chosen to simulate semi-exposed relics akin to those found in the K9801 armour pit, enriches our understanding of salt distribution dynamics in archaeological contexts. As depicted in Fig. 10, the substantial presence of pure $CaSO_4$ crystals on the surface of these bricks serves as a direct representation of the potential salt composition that may accumulate in relics such as those found in the K9801 armour pit.

X-ray diffraction analysis identified these crystals as pure $CaSO_4$. Furthermore, the X-ray diffraction outcomes corroborated the migration of Ca^{2+} on the soil surface, as depicted in Fig. 10c. During the hydration stage, Ca^{2+} was abundant on the soil surface due to its interaction with SO_4^{2-} to form slightly soluble precipitates. Over time, the content of Ca^{2+} ions decreased, mimics conditions that may occur in the K9801 armour pit.

By considering the overall pattern of ion migration in the soil, it can be inferred that some of the SO_4^{2-} originated from the lower layer of the soil column. Additionally, aside from the soil, atmospheric SO_2 was proposed by Dimes F G as another source of the sulfur (S) element. This could explain the presence of SO_4^{2-} ions in the soil system [32]. This external influence could parallel environmental conditions affecting the K9801 armour pit, underscoring the importance of accounting for various factors in comprehending salt.

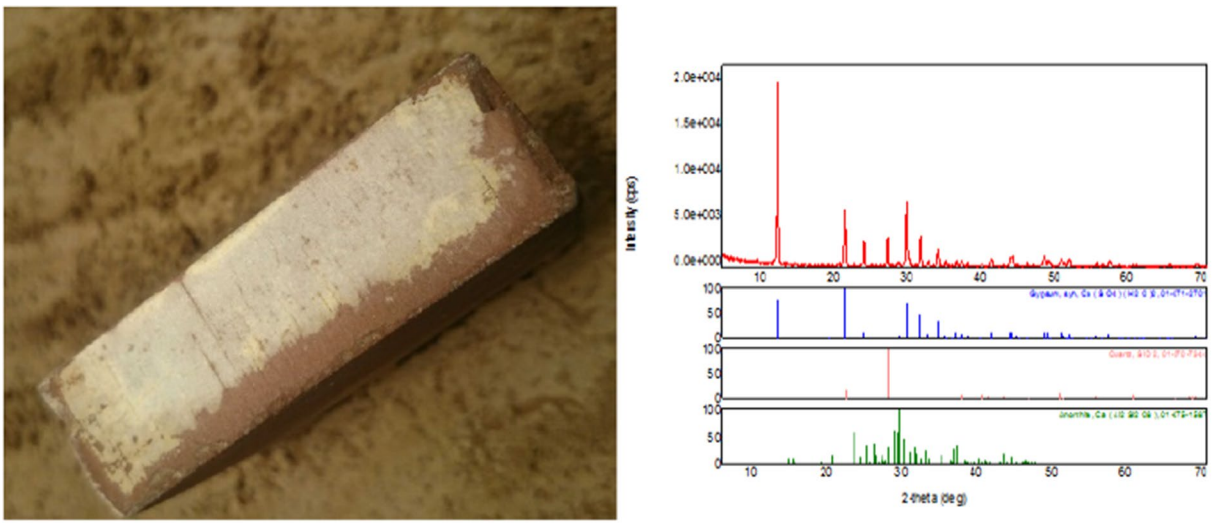

Fig. 10 Soil column brick salt crust and X-ray diffraction pattern

The analysis of salt distribution in the brick samples extracted from different heights within the simulated soil column provides valuable insights into the potential salt enrichment dynamics akin to those observed in the K9801 armour pit. The samples labeled A to D (1-4cm) were obtained from the brick's exposed surface to the air, while the samples E to H (5-8cm) were extracted from the buried sections in the soil column. These samples were analyzed for the presence of Cl^-, NO_3^-, Na^+, Ca^{2+}, and Mg^{2+} ions.

An examination of the plasma image revealed that the salt content of the brick's exposed surface to the air had increased, with ion concentrations exhibiting an upward trend from the bottom to the top of the brick. Specifically, the concentration of Cl^- in the brick's surface area was found to be five times greater than the initial concentration of the brick. This Cl^- concentration decreased gradually as the position moved downward. The buried brick samples exhibited lower Cl^- concentrations, and in fact, sample 5's Cl^- concentration was even lower than that of the Cl^- concentration in the soil on the surface of the soil column after evaporation. The trends for NO_3^-, Na^+, and Ca^{2+} were similar to Cl^-. Their concentrations also increased from the bottom to the top of the brick.

Notably, the salt content inside the brick and on the surface of the soil was lower than the ion concentrations found on the surface of the soil. The migration of Cl^-, NO_3^-, Na^+, and Ca^{2+} from the soil to the brick occurred in conjunction with water movement, with the ions moving upwards along with the water during the migration process. Importantly, the ions did not remain within the soil but continued to travel along the brick's surface. This phenomenon, where higher salt concentration leads to higher osmotic pressure, is consistent with the findings of Luo et al.'s research [5, 6].

Comparing to the K9801 armour pit, which contains similar semi-exposed relics, the analysis of ion concentrations in the simulated brick samples establishes a basis for comprehending potential salt enrichment in archaeological contexts. However, it's vital to recognize the experimental nature of the soil column setup and the necessity for additional research to validate these findings in real-world scenarios.

The enrichment pattern of SO_4^{2-} in the cultural relics differed from that of other ions. The X-ray diffraction results of the salt crystallization on the brick's surface confirmed that the precipitated crystal was $CaSO_4$ (calcium sulfate) (Fig. 10). Interestingly, the concentration of Ca^{2+} was found to be higher closer to the top of the soil brick (Fig. 11). Exploring the mechanisms behind this enrichment, especially in the upper regions of the brick, could offer valuable insights into the specific environmental factors influencing the dynamics of calcium ions in semi-exposed relics.

Furthermore, the enrichment of K^+ ions was predominantly observed in the part of the brick that was exposed to the air. Notably, the closer the enrichment occurred to the surface of the brick, the higher the ion concentration. Taken together, the nuanced enrichment patterns of different ions in the simulated brick samples offer a comprehensive view of the ion dynamics within the semi-exposed relics. While the experiment provides a controlled environment, the parallels drawn with the K9801 armour pit highlight the potential relevance of these findings in understanding the intricate salt migration processes in real-world archaeological contexts.

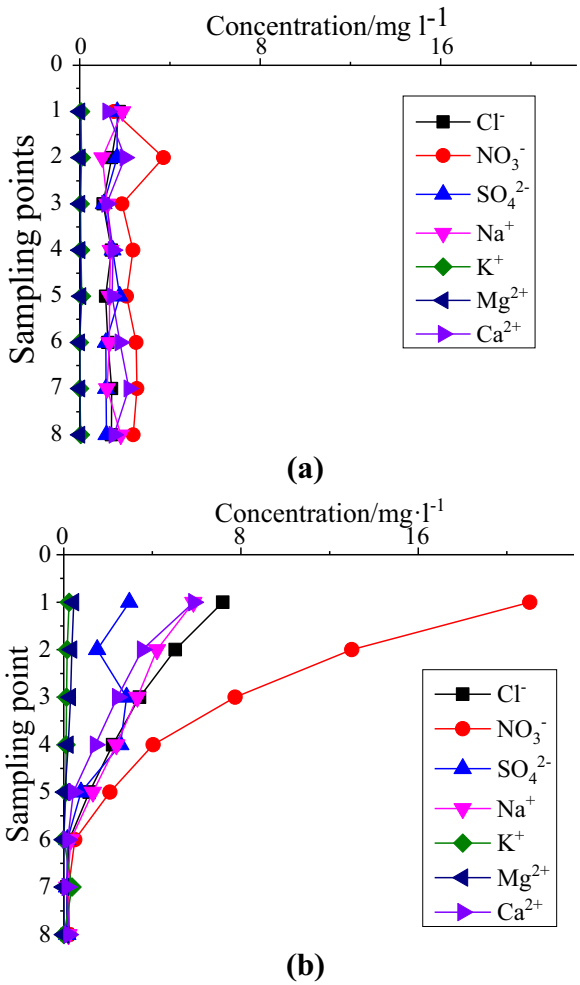

Fig. 11 Comparison of ion distribution in bricks before and after the experiment. **a** before the experiment; **b** after the experiment

Further investigations, both in simulated setups and actual archaeological sites, will be pivotal to refining our understanding of ion interactions and enrichments in semi-exposed relics.

Conclusion

In this study, the investigation of the K9801 Armour pit and the soil column experiment provided insights into the water-salt migration process in semi-exposed relics, leading to the following conclusions:

(1) The soil column experiment demonstrated an effective simulation of salt distribution in semi-exposed relics, highlighting that salt ions were predominantly found within the surface 0–5 cm layer, with lower concentrations in the 20–80 cm depth range. However, variations in the study duration and soil type contributed to notable differences in the distribution of distinct salts between the experimental soil column and the K9801 Armour pit soil.

(2) The vertical migration of soil salinity is influenced by gravity, osmotic pressure, and evaporation. Salt ions tend to migrate towards the surface along with soil moisture, resulting in a reduction of ion content in the layers below the surface. Notably, ions such as Ca^{2+}, Na^{+}, Mg^{2+}, Cl^{-}, and SO_4^{2-} are deposited on the soil surface. The increase in SO_4^{2-} content can be attributed not only to ion migration but also to external factors such as atmospheric SO_2.

(3) Semi-exposed relics have a considerable impact on the migration of soil ions. The process of evaporation leads to significant migration of soil aqueous solution into the brick materials, causing the formation of $CaSO_4$ crystals at higher evaporation rates. This phenomenon can affect the aesthetic appearance of cultural relics.

By combining the findings from the K9801 Armour pit and the soil column experiment, this study offers valuable insights into the complex dynamics of water-salt migration in semi-exposed relics, shedding light on the preservation challenges and strategies for these artifacts.

Author contributions

WY, LX, CB,XY and LJ conceptualized the study. WY and CB were responsible for the methodology, while XY handled the software. The original manuscript draft was written by WY and LX. All authors, namely WY, LX, and LJ, participated in reviewing and editing the manuscript. All authors have read and approved the final version of the manuscript for publication.

Funding

This work was funded by the National Natural Science Foundation of China (52078417).

Availability of data and materials

All data generated or analyzed during this study are included in this published article.

Declarations

Competing interests

The authors declare no competing interests.

Received: 16 October 2023 Accepted: 29 December 2023
Published online: 03 January 2024

References

1. Luo X, Chang B, Tian W, Li J, Gu Z. Experimental study on local environmental control for historical site in archaeological museum by evaporative cooling system. Renew Energ. 2019;143:798–809.
2. Sun M, Shen Y. Research on the actualities and countermeasures of the protection of the earthen sites along the silk road. Res Conserv Cave Temples Earthen Sites. 2022;1(01):70–9.
3. Luo X, Dang Y, Yu CW, Gu Z. The practice of local environment control for the funerary pits of Emperor Qin's Mausoleum Site Museum. Indoor Built Environ. 2021;30(3):293–7.

4. Richards J, Viles H, Guo Q. The importance of wind as a driver of earthen heritage deterioration in dryland environments. Geomorphology. 2020;369:107363.
5. Luo X, Gu Z, Tian W, Xia Y, Ma T. Experimental study of a local ventilation strategy to protect semi-exposed relics in a site museum. Energ Buildings. 2018;159:558–71.
6. Luo X, Gu Z, Yu C. Desiccation cracking of earthen sites in archaeology museum–a viewpoint of chemical potential difference of water content. Indoor Built Environ. 2015;24(2):147–52.
7. Luo X, Song P, Wang Y, Tian W, Gu Z. Design of an energy-saving environmental control system for relics preservation in archaeology museum. Energy Procedia. 2016;104:431–6.
8. Hemeda S. Finite element assessment FEA of polymer anti-seismic piling techniques for protection of the underground culture heritage. Herit Sci. 2022;10(1):35.
9. Yang H, Ni J, Chen C, et al. Weathering assessment approach for building sandstone using hyperspectral imaging technique. Herit Sci. 2023;11(1):1–18.
10. Fasihi H, Kamran DH. The vulnerability of cities' historical fabrics against natural and human-induced hazards: a case study in the pamenar neighbourhood of Tehran. Iran Conserv Manage Archa. 2021;23(1–2):31–41.
11. Gu Z, Luo X, Meng X, Wang Z, Ma T, Yu C, Rong B, Li K, Li W, Tan Y. Primitive environment control for preservation of pit relics in archeology museums of China. Environ Sci Technol. 2013;47(3):1504–9.
12. Kim CS, Chung SJ. Daylighting simulation as an architectural design process in museums installed with toplights. Build Sci. 2011;46(1):210–22.
13. Luo X, Hou Q, Wang Z, Gu Z. Independent preservation environment control for in-situ relics in archaeology museum. Procedia Engg. 2015;121:2217–23.
14. Yue J, Huang X, Zhao L, Wang Z. A stability analysis of the ancient site of liye based on the strength reduction method. Appl Sci. 2022;12(6):2986.
15. Pan C, Chen K, Chen D, Xi S, Geng J, Zhu D. Research progress on in-situ protection status and technology of earthen sites in moisty environment. Constr Build Mater. 2020;253:119219.
16. Cuca B, Agapiou A. Impact of land-use change and soil erosion on cultural landscapes: the case of cultural paths and sites in Paphos district. Cyprus Appl Geomatics. 2018;10(4):515–27.
17. Flatt RJ, Caruso F, Sanchez AMA, Scherer GW. Chemo-mechanics of salt damage in stone. Nat Commun. 2014;5(1):4823.
18. Silverman H, Blumenfield T. Cultural heritage politics in China: an introduction[M]//Cultural heritage politics in China. New York: Springer; 2013.
19. Chang B, Wen H, Yu CW, Luo X, Gu Z. Preservation of earthen relic sites against salt damages by using a sand layer. Indoor Built Environ. 2022;31(4):1142–56.
20. Liu R, Zhang B, Zhang H, Shi M. Deterioration of Yungang Grottoes: diagnosis and research. J Cult Herit. 2011;12(4):494–9.
21. Guo F, Jiang G. Investigation into rock moisture and salinity regimes: implications of sandstone weathering in Yungang Grottoes. China Carbonates Evaporites. 2015;30(1):1–11.
22. Jia Q, Chen W, Tong Y, Guo Q. Experimental study on capillary migration of water and salt in wall painting plastera case study at Mogao Grottoes. China Int J Archit Herit. 2022;16(5):705–16.
23. Zhao J, Luo H, Huang X. Migration, crystallization and dissolution changes of salt solution with color rendering property in porous quartz materials. Mol. 2020;25(23):5708.
24. Arnold A, Zehnder K. Monitoring wall paintings affected by soluble salts[M]. Marina Del Rey: Getty Conservation Institute, 1987;103–135.
25. Steiger M. Crystal growth in porous materials—I: the crystallization pressure of large crystals. J Cryst Growth. 2005;282(3–4):455–69.
26. Russo D. Leaching characteristics of a stony desert soil. Soil Sci Soc Am J. 1983;47(3):431–8.
27. Luo X, Lei S, Tian W, et al. Evaluation of air curtain system orientated to local environmental control of archaeological museum: a case study for the stone armor pit of Emperor Qin's Mausoleum Museum. Sustain Cities Soc. 2020;57:102121.
28. Liao L, Pan C, Yu MA. Manufacturing techniques of armor strips excavated from Emperor Qin Shi Huang's mausoleum. China Trans Nonferrous Met Soc China. 2010;20(3):395–9.
29. Xu J, Li Y, Ren C, Wang S, Vanapalli SK, Chen G. Influence of freeze-thaw cycles on microstructure and hydraulic conductivity of saline intact loess. Cold Reg Sci Technol. 2021;181:103183.
30. Varble J, Chávez J. Performance evaluation and calibration of soil water content and potential sensors for agricultural soils in eastern Colorado. Agric Water Manage. 2011;101(1):93–106.
31. Xia Y, Fu F, Wang J, et al. Salt enrichment and its deterioration in earthen sites in Emperor Qin's Mausoleum Site Museum. China Indoor Built Environ. 2023;32(9):1862–74.
32. Du YJ, Hayashi S, Liu SY. Experimental study of migration of potassium ion through a two-layer soil system. Environ Geol. 2005;48:1096–106.

Publisher's Note